Journal of Physics B: Atomic, Molecular and Optical Physics

PAPER

Enhanced multipartite entanglement via quantum coherence with an atom-assisted optomechanical system

To cite this article: Xihua Yang *et al* 2018 *J. Phys. B: At. Mol. Opt. Phys.* **51** 205501

View the article online for updates and enhancements.

IOP ebooks™

Bringing you innovative digital publishing with leading voices to create your essential collection of books in STEM research.

Start exploring the collection - download the first chapter of every title for free.

This content was downloaded from IP address 59.78.190.9 on 30/11/2018 at 02:56

IOP Publishing Journal of Physics B: Atomic, Molecular and Optical Physics
J. Phys. B: At. Mol. Opt. Phys. **51** (2018) 205501 (9pp) https://doi.org/10.1088/1361-6455/aadf4b

Enhanced multipartite entanglement via quantum coherence with an atom-assisted optomechanical system

Xihua Yang[1], **Jiaqi Liu**[1], **Xiaona Yan**[1] and **Min Xiao**[2]

[1] Department of Physics, Shanghai University, Shanghai 200444, People's Republic of China
[2] Department of Physics, University of Arkansas, Fayetteville, AR 72701, United States of America

E-mail: yangxh@shu.edu.cn

Received 6 August 2018, revised 30 August 2018
Accepted for publication 6 September 2018
Published 25 September 2018

Abstract

We present a scheme to significantly enhance multipartite entanglement with an atom-assisted single-cavity optomechanical system. By embedding an ensemble of Λ-type three-level atoms into the cavity, the stationary tripartite entanglement among two longitudinal cavity modes and a mirror oscillation mode can be greatly enhanced due to quantum coherence induced between the two lower atomic states when one (another) cavity mode is driven at the red (blue) mechanical sideband, and both cavity modes are blue-detuned by the mechanical frequency to the respective atomic resonant transitions; moreover, strong light–light–atom–mirror quadripartite entanglement can also be obtained. The present hybrid system can serve as a promising platform for realizing various quantum protocols, and may find potential applications in quantum information processing and quantum networks.

Keywords: multipartite entanglement, atomic coherence, optomechanical system

(Some figures may appear in colour only in the online journal)

1. Introduction

Multipartite entanglement plays an essential role in quantum computation, quantum communication, and quantum networks [1–3]. How to conveniently and efficiently realize the generation, distribution, storage, retrieval, and manipulation of quantum entanglement is the basic requirement for quantum networks and quantum information processing. The traditionally-employed way for producing multiple entangled light fields is to use polarizing beam splitters to mix the generated squeezed fields through parametric down-conversion processes in nonlinear optical crystals [4]; however, the created entangled fields are normally degenerate, have large bandwidth, and suffer from short correlation time. As is well known, a realistic quantum information network would be composed of many quantum nodes and channels, where multiple entangled fields with narrow bandwidth and different frequencies are required to connect different physical systems at the nodes of quantum networks. The atomic system [5–10] or cavity optomechanical system [11–32] interacting with light fields provides a promising and potential quantum interface for realizing various quantum information protocols, where light fields act as the long-distance quantum information carriers, and the atomic ensemble or vibrating mirror provides an attractive medium for storage and manipulation of quantum information. Comparing with the atomic system which relies on particular frequencies corresponding to naturally existing resonances, the optomechanical system can, in principle, couple to light fields with any frequency, thereby providing a convenient and efficient way for producing entangled fields with any desired wavelengths; in addition, the optomechanical system can also be used to explore quantum features at the mesoscopic or even macroscopic scale [12, 32].

Recently, the combination of the atomic system and cavity optomechanical system has been extensively examined to generate atom–mirror–light multipartite entanglement [14–17]. Genes [14] investigated the tripartite entanglement among the atoms, cavity field, and moving mirror with a cavity optomechanical system filled with a two-level atomic

 © 2018 IOP Publishing Ltd Printed in the UK

medium, where the cavity field is resonant with the anti-Stokes sideband of the input laser field, and a significant atom–light–mirror entanglement is obtained. Ian [15] has shown that the atoms can effectively enhance the radiation pressure of the cavity field on the vibrating mirror generating an atom–light–mirror tripartite entanglement in an optomechanical cavity containing a two-level atomic ensemble. Hammerer [16] proposed a scheme for the creation of a robust Einstein–Podolsky–Rosen-type of entanglement between the nanomechanical resonator and atomic ensembles mediated by a laser field. Zhou [17] studied the atomic-coherence-induced entanglement between the two-mode fields, as well as two optomechanical oscillators with the ladder-type three-level atoms embedded in an optomechanical cavity.

Here, by using the atom-assisted single-cavity optomechanical system, we show that the light–mirror–light tripartite entanglement can be dramatically enhanced due to quantum coherence induced between the lower doublet of the Λ-type three-level atoms in contrast to the case without atoms in the cavity when the first (second) input laser field is tuned to the red (blue) sideband of the mechanical oscillator; moreover, strong quadripartite entanglement among the two cavity fields, vibrating mirror, and atoms can be established. Note that the present scheme for generating multipartite entanglement is quite distinct as compared to that in [14, 17]. In [14], the entanglement among the short-lived electronically excited states of an atomic ensemble and a nanomechanical system was investigated, and it is shown that entanglement sharing would exist among the subsystems, whereas here we employ the Λ-type three-level atomic system and study the entanglement among the long-lived lower doublet of the atoms, two cavity fields, and vibrating mirror, which is vital for the quantum repeater application. In [17], the authors employed a dual-cavity optomechanical system to entangle two cavity fields as well as two optomechanical oscillators via atomic coherence by injecting the ladder-type three-level atoms into the cavity, where the bipartite entanglement between the two separated movable mirrors results from the transfer of entanglement between the two cavity fields, which can not be produced through the pure optomechanical interaction (without atoms). Instead, here we show that by using the atom-assisted single-cavity optomechanical system, dramatic enhancement of the stationary tripartite entanglement among two cavity fields and a movable mirror can be obtained due to quantum coherence between the lower doublet of the Λ-type three-level atoms, where both the optomechanical interaction and atom-field coupling have contributions to the multipartite entanglement generation; moreover, as the two cavity fields are significantly entangled by their common interaction with the mechanical resonator as well as the atoms, strong light–light–atom–mirror quadripartite entanglement can also be obtained.

2. Theoretical model and Heisenberg–Langevin equations

The considered hybrid system, as shown in figure 1(a), consists of an ensemble of N atoms (e.g. ^{85}Rb) confined inside an optical Fabry–Perot cavity with one partially transmitting fixed mirror and another perfectly reflecting vibrating mirror with oscillation frequency ω_m and mechanical damping rate γ_m. The atom-assisted cavity optomechanical system is driven by two input laser fields with frequencies ω_{L1} and ω_{L2} coupling two neighboring longitudinal cavity modes with frequencies ω_{a1} and ω_{a2}, and the two cavity fields simultaneously couple the atomic electric dipole transitions $|1\rangle$-$|3\rangle$ and $|2\rangle$-$|3\rangle$, respectively. The relevant energy level scheme of the Λ-type three-level atoms and the corresponding two input driving and cavity fields are displayed in figure 1(b). In this case, the total Hamiltonian of the hybrid system can be written as [11, 15–17]

$$\begin{aligned} H &= \hbar\omega_{a1}a_1^{+}a_1 + \hbar\omega_{a2}a_2^{+}a_2 + \hbar\omega_m(p^2+q^2) \\ &+ i\hbar\eta_1(a_1^{+}e^{-i\omega_{L1}t} - a_1e^{i\omega_{L1}t}) + i\hbar\eta_2(a_2^{+}e^{-i\omega_{L2}t} - a_2e^{i\omega_{L2}t}) \\ &- \hbar g_1a_1^{+}a_1q - \hbar g_2a_2^{+}a_2q + \hbar\omega_1\sigma_{11} + \hbar\omega_2\sigma_{22} \\ &+ \hbar\omega_3\sigma_{33} + (\hbar g_{13}\sqrt{N}a_1^{+}\sigma_{13} + \hbar g_{23}\sqrt{N}a_2^{+}\sigma_{23} + \text{H.c.}), \end{aligned} \tag{1}$$

where a_1 (a_1^{+}) and a_2 (a_2^{+}) are the annihilation (creation) operators of the two cavity field modes 1 and 2 with decay rates κ_1 and κ_2, respectively; q and p are the dimensionless position and momentum operators of the vibrating mirror; $g_{1,2} = \omega_{a1,a2}\sqrt{\hbar/m\omega_m}/L$ is the optomechanical coupling coefficient of the radiation pressure with L being the cavity length, and m the effective mass of the mechanical oscillator; the two terms involving η_1 and η_2 describe the interactions of the input driving laser fields with the two cavity modes and $\eta_{1(2)}$ is related to the input field power $P_{1(2)}$ with $\eta_{1(2)} = \sqrt{2P_{1(2)}\kappa/\hbar\omega_{L1(L2)}}$ (here we assume $\kappa_1 = \kappa_2 = \kappa$ for simplicity); $\sigma_{ab} = \frac{1}{\sqrt{N}}\sum_{i=1}^{N}\sigma_{ab}^{(i)}(a \neq b,\ a, b = 1, 2, 3)$ and $\sigma_{aa} = \sum_{i=1}^{N}\sigma_{aa}^{(i)}$ are the collective operators of the atomic ensemble, $g_{13(23)} = \mu_{13(23)}\cdot\varepsilon_{1(2)}/\hbar$ is the atom-field coupling constant with $\mu_{13(23)}$ being the dipole moment for the 1-3 (2-3) transition and $\varepsilon_{1(2)} = \sqrt{\hbar\omega_{a1(a2)}/2\varepsilon_0V}$ as the electric field of the cavity field photon with V being the cavity mode volume. We denote the frequency detunings of the two cavity fields 1 and 2 with respect to the corresponding input laser fields (the atomic 1-3 and 2-3 transitions) as $\Delta_{c1} = \omega_{a1} - \omega_{L1}$ and $\Delta_{c2} = \omega_{a2} - \omega_{L2}$ ($\Delta_1 = \omega_{a1} - \omega_{31}$ and $\Delta_2 = \omega_{a2} - \omega_{32}$), respectively. By transforming the cavity field 1 (2) and the atomic operator σ_{13} (σ_{23}) to a rotating frame at the input field frequency ω_{L1} (ω_{L2}), the Heisenberg–Langevin equations of the hybrid system can be rewritten as

$$\dot{q} = \omega_m p, \tag{2a}$$

$$\dot{p} = -\omega_m q - \gamma_m p + g_1a_1^{+}a_1 + g_2a_2^{+}a_2 + \xi, \tag{2b}$$

$$\begin{aligned} \dot{a}_1 &= -(\kappa_1 + i\Delta_{c1})a_1 + ig_1a_1q + \eta_1 - ig_{13}\sqrt{N}\sigma_{13} \\ &+ \sqrt{2\kappa_1}a_1^{in}, \end{aligned} \tag{2c}$$

$$\begin{aligned} \dot{a}_2 &= -(\kappa_2 + i\Delta_{c2})a_2 + ig_2a_2q + \eta_2 - ig_{23}\sqrt{N}\sigma_{23} \\ &+ \sqrt{2\kappa_2}a_2^{in}, \end{aligned} \tag{2d}$$

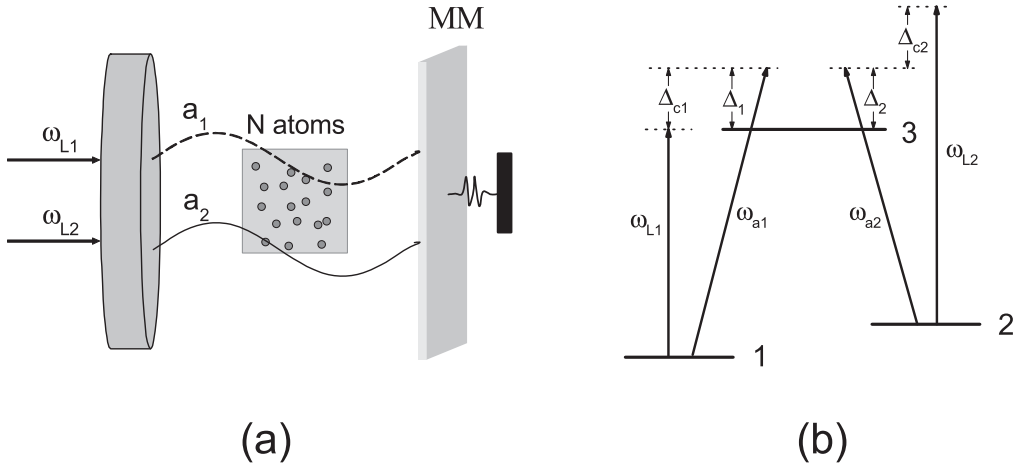

Figure 1. (a) The atom-assisted cavity optomechanical system with N atoms and a movable mirror (MM) driven by two input laser fields with frequencies ω_{L1} and ω_{L2}, where a_1 and a_2 represent the two longitudinal cavity field modes with frequencies ω_{a1} and ω_{a2}, respectively. (b) The relevant energy level scheme of the Λ-type three-level atoms and the corresponding two input driving and cavity fields.

$$\dot{\sigma}_{12}(t) = -[\gamma_{12} + i(\Delta_{c1} - \Delta_1 + \Delta_2 - \Delta_{c2})]\sigma_{12} + ig_{13}a_1\sigma_{32} - ig_{23}a_2^{+}\sigma_{13} + F_{12}, \quad (2e)$$

$$\dot{\sigma}_{13}(t) = -[\gamma_{13} + i(\Delta_{c1} - \Delta_1)]\sigma_{13} - ig_{13}a_1(\sigma_{11} - \sigma_{33})/\sqrt{N} - ig_{23}a_2\sigma_{12} + F_{13}, \quad (2f)$$

$$\dot{\sigma}_{23}(t) = -[\gamma_{23} + i(\Delta_{c2} - \Delta_2)]\sigma_{23} - ig_{23}a_2(\sigma_{22} - \sigma_{33})/\sqrt{N} - ig_{13}a_1\sigma_{21} + F_{23}, \quad (2g)$$

where $a_{1,2}^{in}(t)$ and $\xi(t)$ are the optical and mechanical noise operators with the relevant nonzero correlation functions $\langle a_{1,2}^{in}(t)a_{1,2}^{in+}(t')\rangle = \delta(t-t')$ and $\langle \xi(t)\xi(t') + \xi(t')\xi(t)\rangle/2 = \gamma_m(2\overline{n}+1)\delta(t-t')$ in the limit of large mechanical quality factor (i.e., $Q_m = \omega_m/\gamma_m \gg 1$ [18]), where $\overline{n} = 1/(\exp(h\omega_m/k_BT) - 1)$ is the mean thermal phonon number with k_B being the Boltzmann constant and T the mirror temperature, $\gamma_{13} = \gamma_{23} = \frac{\gamma_1+\gamma_2}{2}$ with γ_1 and γ_2 being the population decay rates from level 3 to levels 1 and 2, respectively, γ_{12} is the coherence decay rate between levels 1 and 2, and $F_{ij}(t)$ are the collective atomic δ-correlated Langevin noise operators. As done in [8], we assume that the atoms are initially prepared in a coherent state in the Λ-type electromagnetically induced transparency (EIT) configuration resonantly driven by another two strong coherent pump and probe fields with Rabi frequencies Ω_c and Ω_p ($\Omega_c \gg \Omega_p$) far larger than $g_{13}\sqrt{N}\alpha_1$ and $g_{23}\sqrt{N}\alpha_2$ (α_1 and α_2 being the steady-state mean values of the cavity fields 1 and 2), respectively, so the two cavity fields have negligible influence on the atomic coherence and population. Under these conditions, the collective atomic spin coherence σ_{21} can be viewed as approximately satisfying the bosonic commutation relation $[\sigma_{21}, \sigma_{12}] = (\sum_i|2\rangle_{i_i}\langle 2| - \sum_i|1\rangle_{i_i}\langle 1|)/N \approx 1$, therefore, the produced atomic spin coherence σ_{21} can be treated as a bosonic field. We use the similar perturbation analysis as that in [8, 17] to treat the interaction of the atoms with the two cavity fields. In the zeroth-order perturbation expansion, by semiclassically treating the interaction of the atoms with the strong coupling and probe fields in the Λ-type EIT configuration, one can get the steady-state mean values of the atomic operators $\sigma_{11}^{(0)}$, $\sigma_{22}^{(0)}$, $\sigma_{33}^{(0)}$, $\sigma_{12}^{(0)}$, $\sigma_{13}^{(0)}$, and $\sigma_{32}^{(0)}$ [8]. By substituting the zeroth-order solution of the atomic operators into equations (2*e*)–(2*g*), the first-order solution $\sigma_{12}^{(1)}$, $\sigma_{13}^{(1)}$, and $\sigma_{23}^{(1)}$ can be obtained. We assume that $\gamma_1, \gamma_2 \gg \kappa, \gamma_m, \gamma_{12}$, so the atomic operators $\sigma_{13}^{(1)}$ and $\sigma_{23}^{(1)}$ can be adiabatically eliminated. Substituting $\sigma_{13}^{(1)}$ and $\sigma_{23}^{(1)}$ into equations (2*c*) and (2*d*), respectively, one can get the evolution equations of the operators a_1 and a_2. By writing each Heisenberg operator as the sum of its steady-state mean value and a small fluctuation operator with zero-mean value, and defining the cavity field quadratures $\delta X_{1,2} = (\delta a_{1,2} + \delta a_{1,2}^{+})/\sqrt{2}$ and $\delta Y_{1,2} = (\delta a_{1,2} - \delta a_{1,2}^{+})/\sqrt{2}\,i$ with the corresponding Hermitian input noise operators $X_{1,2}^{in} = (a_{1,2}^{in} + a_{1,2}^{in+})/\sqrt{2}$ and $Y_{1,2}^{in} = (a_{1,2}^{in} - a_{1,2}^{in+})/\sqrt{2}\,i$, as well as the atomic quadratures $\delta X_s = (\delta\sigma_{12}^{(1)} + \delta\sigma_{21}^{(1)})/\sqrt{2}$ and $\delta Y_s = (\delta\sigma_{21}^{(1)} - \delta\sigma_{12}^{(1)})/\sqrt{2}\,i$ with the corresponding Hermitian noise operators $X_s^{in} = (F_{21} + F_{12})/\sqrt{2}$ and $Y_s^{in} = (F_{21} - F_{12})/\sqrt{2}\,i$, respectively, we can obtain the quantum Langevin equations for the fluctuation operators as follows:

$$\delta\dot{q} = \omega_m\delta p, \quad (3a)$$

$$\delta\dot{p} = -\omega_m\delta q - \gamma_m\delta p + \sqrt{2}\,g_1\alpha_1\delta X_1 + \sqrt{2}\,g_2\alpha_2\delta X_2 + \xi, \quad (3b)$$

$$\delta\dot{X}_1 = -\kappa_1\delta X_1 + (\Delta_{c1} - g_1q_s)\delta Y_1 + \mathrm{Re}\,k_{11}\delta X_1 - \mathrm{Im}k_{11}\delta Y_1 + \mathrm{Re}\,k_{12}\delta X_2 - \mathrm{Im}k_{12}\delta Y_2 + \sqrt{2\kappa_1}\delta X_1^{in}, \quad (3c)$$

$$\delta\dot{Y}_1 = -\kappa_1\delta Y_1 - (\Delta_{c1} - g_1q_s)\delta X_1 + \sqrt{2}\,g_1\alpha_1\delta q + \mathrm{Re}\,k_{11}\delta Y_1 + \mathrm{Im}k_{11}\delta X_1 + \mathrm{Re}\,k_{12}\delta Y_2 + \mathrm{Im}k_{12}\delta X_2 + \sqrt{2\kappa_1}\delta Y_1^{in}, \quad (3d)$$

$$\delta\dot{X}_2 = -\kappa_2\delta X_2 + (\Delta_{c2} - g_2q_s)\delta Y_2 + \mathrm{Re}\,k_{22}\delta X_2 - \mathrm{Im}k_{22}\delta Y_2 + \mathrm{Re}\,k_{21}\delta X_1 - \mathrm{Im}k_{21}\delta Y_1 + \sqrt{2\kappa_2}\delta X_2^{in}, \quad (3e)$$

$$\delta\dot{Y}_2 = -\kappa_2\delta Y_2 - (\Delta_{c2} - g_2q_s)\delta X_2 + \sqrt{2}\,g_2\alpha_2\delta q + \mathrm{Re}\,k_{22}\delta Y_2 + \mathrm{Im}k_{22}\delta X_2 + \mathrm{Re}\,k_{21}\delta Y_1 + \mathrm{Im}k_{21}\delta X_1 + \sqrt{2\kappa_2}\delta Y_2^{in}, \quad (3f)$$

$$\delta\dot{X}_s = -\gamma_{12}\delta X_s - (\Delta_{c1} - \Delta_1 + \Delta_2 - \Delta_{c2})\delta Y_s + \mathrm{Re}\,k_1\delta X_1 - \mathrm{Im}k_1\delta Y_1 + \mathrm{Re}\,k_2\delta X_2 + \mathrm{Im}k_2\delta Y_2 + \sqrt{2\gamma_{12}}X_s^{in}, \quad (3g)$$

$$\delta\dot{Y}_s = -\gamma_{12}\delta Y_s + (\Delta_{c1} - \Delta_1 + \Delta_2 - \Delta_{c2})\delta X_s - \mathrm{Re}\,k_1\delta Y_1 - \mathrm{Im}k_1\delta X_1 + \mathrm{Re}\,k_2\delta Y_2 - \mathrm{Im}k_2\delta X_2 + \sqrt{2\gamma_{12}}Y_s^{in}. \quad (3h)$$

In the above equations, $k_{11} = \frac{-Ng_{13}^2}{\gamma_{13}+i(\Delta_{c1}-\Delta_1)}(\sigma_{11}^{(0)} - \sigma_{33}^{(0)})$, $k_{12} = \frac{-Ng_{13}g_{23}\sigma_{12}^{(0)}}{\gamma_{13}+i(\Delta_{c1}-\Delta_1)}$, $k_{22} = \frac{-Ng_{23}^2}{\gamma_{23}+i(\Delta_{c2}-\Delta_2)}(\sigma_{22}^{(0)} - \sigma_{33}^{(0)})$, $k_{21} = \frac{-Ng_{13}g_{23}\sigma_{21}^{(0)}}{\gamma_{23}+i(\Delta_{c2}-\Delta_2)}$, $k_1 = -i\sqrt{N}g_{13}\sigma_{32}^{(0)}$, and $k_2 = -i\sqrt{N}g_{23}\sigma_{13}^{(0)}$. Using the similar treatment as in [17] by linearization approximation, calculating equations (2*e*)–(2*g*) to the first order in g_{13} and g_{23} and combining with equations (2*a*)–(2*d*), we can get $\alpha_1^2 = \frac{\eta_1^2}{\kappa_1^2+\Delta_{eff}^2}$, $\alpha_2^2 = \frac{\eta_2^2}{\kappa_2^2+(\Delta_{eff}+2g_1q_s)^2}$, and $q_s = g_1(\alpha_1^2 + \alpha_2^2)/\omega_m$ with $\Delta_{eff} = \Delta_{c1} - g_1q_s$ being the effective detuning of the cavity field 1 with respect to the input laser field 1, where we assume that $\alpha_1/\alpha_2 = \Omega_1/\Omega_2$, $\Delta_{c2} = -\Delta_{c1}$, and choose the phase reference of the driving fields so that α_1 and α_2 are real and positive. The linearized quantum Langevin equations equations (3*a*)–(3*h*) for the fluctuation operators can be written in the following compact form:

$$\dot{u}(t) = Au(t) + n(t), \quad (4)$$

where $u^T(t) = (\delta q(t), \delta p(t), \delta X_1(t), \delta Y_1(t), \delta X_2(t), \delta Y_2(t), \delta X_s(t), \delta Y_s(t))$is the column vector of the fluctuations, $n^T(t) = (0, \xi(t), \sqrt{2\kappa_1}\delta X_1^{in}(t), \sqrt{2\kappa_1}\delta Y_1^{in}(t), \sqrt{2\kappa_2}\delta X_2^{in}(t), \sqrt{2\kappa_2}\delta Y_2^{in}(t), \sqrt{2\gamma_{12}}\delta X_s^{in}(t), \sqrt{2\gamma_{12}}\delta Y_s^{in}(t))$ is the column vector of the noises, and the drift matrix A can be easily obtained from the coefficients of equations (3*a*)–(3*h*). We investigate the steady-state entanglement of the hybrid system formed by the two cavity fields, vibrating cavity mirror, and atoms. The system is stable and reaches its steady state when all of the eigenvalues of drift matrix A have negative real parts. It is difficult to obtain the analytic solution of the the eigenvalues of drift matrix A, so we resort to numerical method to ensure the stability conditions. When the system is in the steady state, the covariance matrix of the quantum fluctuations $V_{ij} = (\langle u_i(\infty)u_j(\infty) + u_j(\infty)u_i(\infty)\rangle)/2$, which characterizes the quantum corrections of any bipartite subsystems, satisfies the Lyapunov equation $AV + VA^T = -D$ [33], where $D = \mathrm{Diag}(0, \gamma_m(2\bar{n}+1), \kappa_1, \kappa_1, \kappa_2, \kappa_2, \gamma_{12}, \gamma_{12})$ is the noise correlation matrix. We can quantify the entanglement of any bipartite subsystems by using the logarithmic negativity E_N, which can be defined as $E_N = \max[0, -\ln 2\eta^-]$ [34], where η^- is the lowest symplectic eigenvalue of the partially transposed covariance matrix associated with the selected bipartition. $E_N > 0$ means the generation of genuine entanglement, and the larger value of the logarithmic negativity E_N, the stronger entanglement can be obtained. We denote the logarithmic negativities for the mirror-atom, atom-field 1 (2), mirror-field 1 (2), and field 1-field 2 as E_N^{ma}, $E_N^{af1(2)}$, $E_N^{mf1(2)}$, and E_N^{f1f2}, respectively. In the following, we consider the parameters of the hybrid system analogous to those of the experimental set-up of [35], which have also been used in the theoretical paper [17]. According to [16, 35], the relevant parameters are set as $L = 0.025$ m, $T = 200\ \mu$K, $\omega_m = 2\pi \times 10^7$ Hz, $\gamma_m = 2\pi \times 140$ Hz, $\kappa = 2\pi \times 2.15 \times 10^5$ Hz, $\lambda = 780$ nm, $m = 145 \times 10^{-12}$ kg, $P = 60$ mW, $\Delta_{c1} = -\Delta_{c2}$, $\Delta_1 = \Delta_2 = \omega_m$, and $N = 1 \times 10^4$, whereas in [17], the oscillation frequency is set to be the largest value available in [35].

3. Results and discussions

Figure 2(a) shows the behavior of entanglement among the two cavity fields, vibrating mirror, and atoms tested by logarithmic negativity E_N as a function of the normalized effective detuning Δ_{eff}/ω_m. It is clear that, E_N^{ma} has nonzero positive values in a limited range of detuning around $\Delta_{eff} = \omega_m$ with a peak value of about 0.174, which means that bipartite entanglement between the vibrating mirror and atoms can be generated although there is no direct coupling between them; the bipartite entanglement between the cavity field 1 and atoms or mirror can exist in a relatively large range of detuning around $\Delta_{eff} = \omega_m$ with peak values of being about 0.182 (note that E_N^{af1} and E_N^{mf1} nearly have the same behavior in the region of chosen parameters, so in order to see clearly, we set the data of E_N^{mf1} to be enlarged by 1.1 times as denoted by the arrows and annotations in the figures 2(a) and (A), and the other arrows and annotations have the similar features). However, E_N^{f1f2}, E_N^{mf2}, and E_N^{af2} have very large nonzero positive values in a wide range of the detuning Δ_{c1} and exhibit robustness to the variation of the effective detuning Δ_{eff} (though they gradually decrease with increasing Δ_{eff}), which demonstrates that high degree of bipartite entanglement between the two cavity fields as well as between the cavity field 2 and mirror (or atoms) are generated. Clearly, as seen in figure 2(a), in the limited detuning range around $\Delta_{eff} = \omega_m$, E_N^{ma}, $E_N^{af1(2)}$, $E_N^{mf1(2)}$, and E_N^{f1f2} are all larger than zero, which indicates that the two cavity fields, vibrating cavity mirror, and atoms are genuinely entangled with each other. For comparison, we show in figure 2(b) the optomechanical entanglement among the two cavity fields and vibrating mirror in the absence of atoms in the cavity and in figure 2(c) the tripartite entanglement among the two cavity fields and atoms with two fixed cavity mirrors. It can be seen from figure 2(b) that E_N^{mf2}, E_N^{f1f2}, and E_N^{mf1} all have nonzero positive values in a narrow range of detuning around $\Delta_{eff} = \omega_m$ with peak values of about $2.4 \times 10^{-3}, 1.9 \times 10^{-4}$, and 4.2×10^{-5}, respectively, where the relative strong bipartite entanglement between the cavity field 2 and mirror results from their parametric-type interaction. Note that the similar scheme with a mechanical resonator interacting simultaneously with two cavity fields has been examined for generating tripartite entanglement in [19, 25] with one (another) cavity mode driven at the red (blue) mechanical sideband, and we use the same parameters as those in [19] to investigate the degree of entanglement among the two cavity fields and mirror and find that nearly the same order of the logarithmic negativity E_N as that in [19] can be obtained, which is much larger than that in figure 2(b) due to the far larger cooperativity C in [19]. Note also that in figure 2(b) the

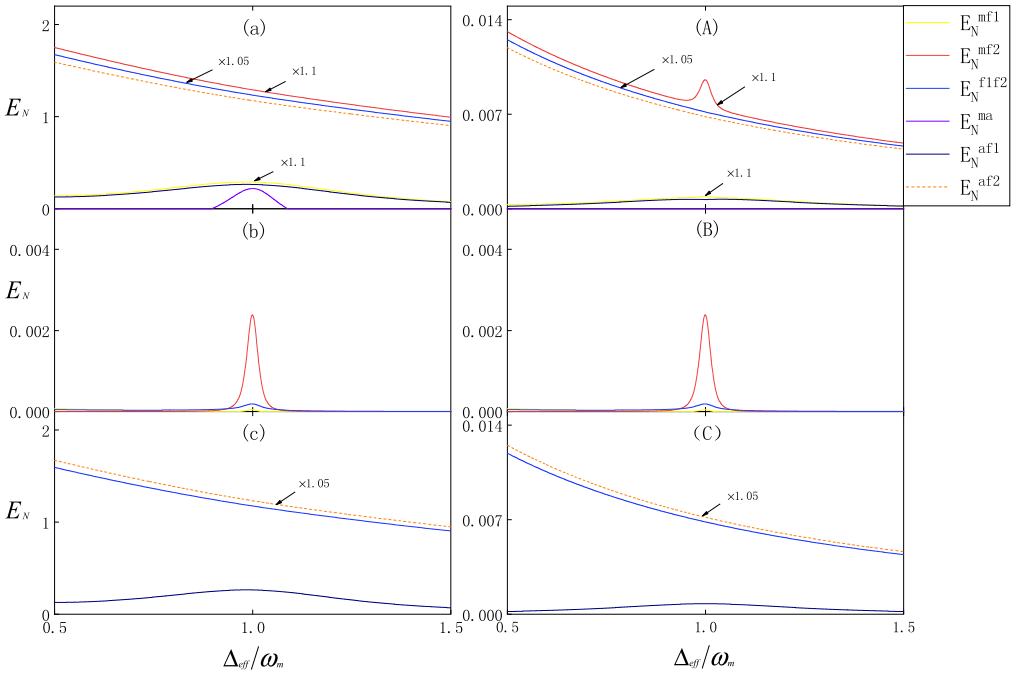

Figure 2. (a) Logarithmic negativity E_N^{ma}, $E_N^{af1(2)}$, $E_N^{mf1(2)}$, and E_N^{f1f2} versus the normalized effective detuning Δ_{eff}/ω_m with $N = 1 \times 10^4$. (b) Logarithmic negativity E_N^{mf1}, E_N^{mf2}, and E_N^{f1f2} versus the normalized effective detuning Δ_{eff}/ω_m without atoms in the cavity. (c) Logarithmic negativity E_N^{af1}, E_N^{af2}, and E_N^{f1f2} versus the normalized effective detuning Δ_{eff}/ω_m with two fixed cavity mirrors. For comparison, (A)–(C) are the same as (a)–(c) but for a different ensemble number $N = 30$.

tripartite entanglement only exists in a narrow range of detuning around $\Delta_{eff} = \omega_m$ as compared to that in [19], which is due to the fact that in our case, the detuning of the cavity field 2 with respect to the input laser field 2 is simultaneously varied with the detuning of the cavity field 1 with respect to the input laser field 1 while keeping $\Delta_{c2} = -\Delta_{c1}$, whereas in [19, 25], only one detuning is varied while anther one is fixed at around ω_m. In addition, as displayed in figure 2(c), there is no apparent variation of the degree of the tripartite entanglement among the two cavity fields and atoms as compared to that in figure 2(a). This is due to the fact that, in the present scheme, the two cavity fields are significantly entangled by their common interaction with the mechanical resonator as well as the atoms; however, as the bipartite entanglement between the two cavity fields resulting from the interaction with the atoms is much stronger than that from the interaction with the mirror (see figures 2(b) and (c)), dramatic enhancement of the tripartite entanglement among the two cavity fields and mirror with the presence of the atoms in the cavity can be realized as compared to that without atoms, whereas nearly no apparent variation of the tripartite entanglement among the two cavity fields and atoms can be observed.

In order to see clearly the effect of the movable mirror (atoms) on the atom-cavity (cavity-mirror) entanglement, we show in figures 2(A)–(C) the behavior of multipartite entanglement versus the normalized effective detuning Δ_{eff}/ω_m with a different ensemble number ($N = 30$) as compared to that in figures 2(a)–(c). Obviously, as shown in figures 2(A)–(C), when the ensemble number N is decreased, i.e., the atom-field coupling strength is reduced, the overall multipartite entanglement would be weakened as compared to figures 2(a)–(c), and nearly no atom–mirror bipartite entanglement can be generated. Comparing figure 2(A) with figure 2(B), it can be seen that significant enhancement of the tripartite entanglement among the two cavity fields and mirror can be also obtained with the presence of the atoms; as compared to figure 2(a), the contribution to the enhancement of the bipartite entanglement between the cavity field 2 (field 1) and mirror from the optomechanical interaction becomes more apparent in figure 2(A), as evidenced by the two additional narrow peaks around $\Delta_{eff} = \omega_m$. Moreover, comparing figures 2(A) with 2(C), it is found that there is a slight decrease of the degree of the tripartite entanglement among the two cavity fields and atoms with a movable mirror, and detailed calculations show that the less the ensemble number is, the more apparent the decrease of the degree of the tripartite entanglement becomes in figure 2(A) with respect to that in figure 2(C).

Figure 3 displays the entanglement among the two cavity fields, the oscillating mirror, and the atoms with respect to the environmental temperature T and the quality factor (Q_m) of the vibrating mirror mode, where in order to maintain the same level of sideband resolution, we assume the quality factor (Q) of the cavity simultaneously varies with the variation of Q_m with $Q = 2.5 \times 10^4 Q_m$. As seen from the 3D plots of the behavior of logarithmic negativity E_N, all of E_N^{ma}, $E_N^{af1(2)}$, $E_N^{mf1(2)}$, and E_N^{f1f2} would increase with the increase of the quality factors of the cavity and vibrating mirror mode within the region of the chosen parameters, that is, the quadripartite entanglement among the two cavity fields,

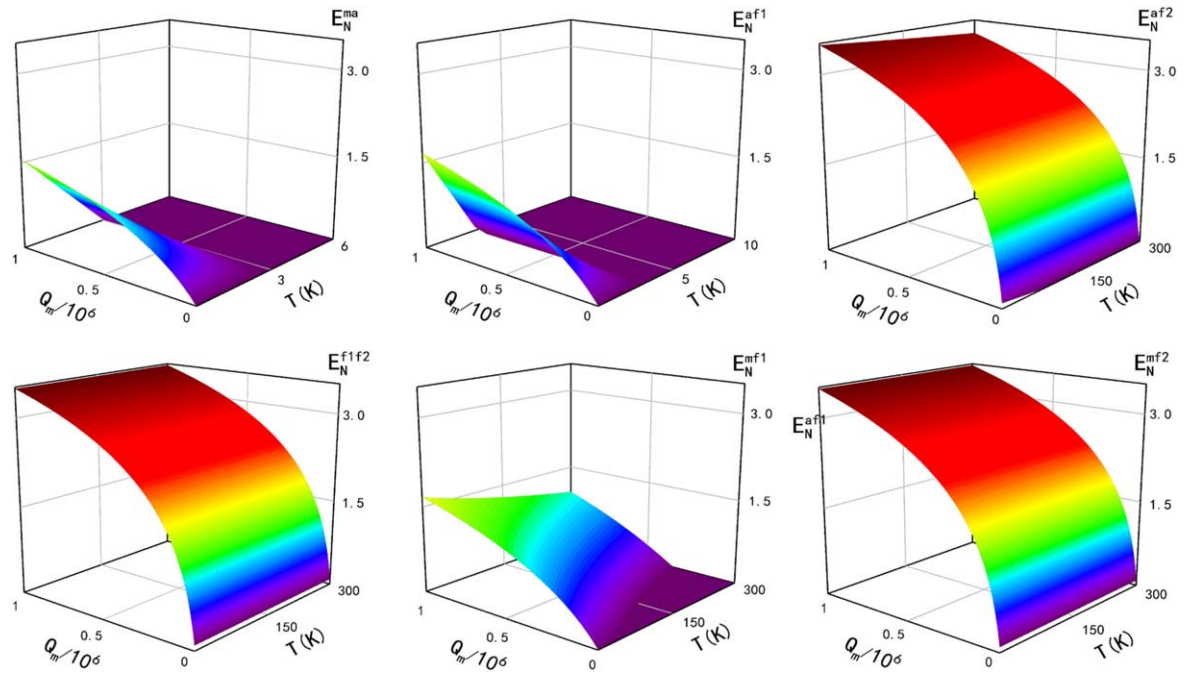

Figure 3. The 3D plots of the behavior of logarithmic negativity E_N^{ma}, $E_N^{af1(2)}$, $E_N^{mf1(2)}$, and E_N^{f1f2} with respect to the environmental temperature T and the quality factor Q_m of the vibrating mirror, where we set $\Delta_{c1} = -\Delta_{c2} = \omega_m$ and $Q = 2.5 \times 10^4 Q_m$, and the other parameters are the same as those in figure 2(a).

mirror, and atoms would be strengthened by increasing the two quality factors Q_m and Q. The bipartite entanglement between the atoms and the mirror would only exist at relatively low environmental temperature and decrease quickly with the increase of the temperature; though the bipartite entanglement between the cavity field 1 and the atoms would be weakened dramatically with the increase of the temperature, it still persists for the temperature above tens of Kelvin with experimentally accessible high-Q mechanical resonator and optical cavity; however, the bipartite entanglements between the two cavity fields, between the cavity field 2 and atoms (or mirror), as well as between the cavity field 1 and mirror exhibit strong robustness to the environmental temperature, and even at room or higher temperature, high degree of entanglement can still be obtained. Clearly, the present hybrid system provides a convenient and efficient quantum interface for quantum information processing.

It is well known that the atomic number N and dephasing rate γ_{12} of the atomic lower doublet play a key role in the generation of entanglement in the Λ-type atomic system [5–10]. In figure 4, we present the dependence of the entanglement among the two cavity fields, oscillating mirror, and atoms on the atomic number N and the dephasing rate γ_{12}. It can be seen that all of E_N^{ma}, $E_N^{af1(2)}$, $E_N^{mf1(2)}$, and E_N^{f1f2} will increase with the increase of the atomic number in the interaction volume within the chosen parameter regime, that is, the degree of the quadripartite entanglement would be enhanced by increasing the atomic number in the cavity. In addition, all of the bipartite entanglements exhibit robustness to the variation of the dephasing rate γ_{12} in the chosen parameter range, which is quite distinct as compared to the bipartite entanglements between the two laser fields as well as between the laser fields and atoms in the free space [8], where the degree of the bipartite entanglements would be dramatically weakened with the increase of the coherence decay rate γ_{12}. Note that when the dephasing rate γ_{12} becomes relatively large and comparable to or larger than the decay rate $\gamma_1(\gamma_2)$ of the excited state, the approximation of the adiabatic elimination of $\sigma_{13,23}$ and the neglect of the depletions of the pump and probe fields would break down, and the multipartite entanglement would be weakened.

To get a physical insight into the enhancement of the tripartite entanglement among the two cavity fields and mechanical oscillator as well as the strong light–light–atom–mirror quadripartite entanglement in the above experimental accessible parameter regime, it is instructive to consider the interaction between the two cavity fields, cavity mirror, and atoms. In the case without atoms in the cavity, when the cavity field 1 (2) is driven at the red (blue) mechanical sideband, the radiation pressure of the input laser beams, impinging on the mechanical oscillator, produces optomechanical coupling between the vibrational mode and two cavity fields, and subsequently results in the tripartite entanglement among the two cavity fields and the mirror. As analyzed in [11, 22, 23], the tripartite entanglement is realized in two steps: the parametric-type interaction of the cavity mode 2 with the mirror oscillation mode produces the bipartite entanglement between the cavity field 2 and mirror, and the beam-splitter-type interaction between the cavity field 1 and mirror maps the state of the entangled phonons in the mechanical oscillator onto photons in cavity field 1, thereby generating tripartite entanglement among the two cavity modes and mirror oscillation mode. In fact, the cavity field

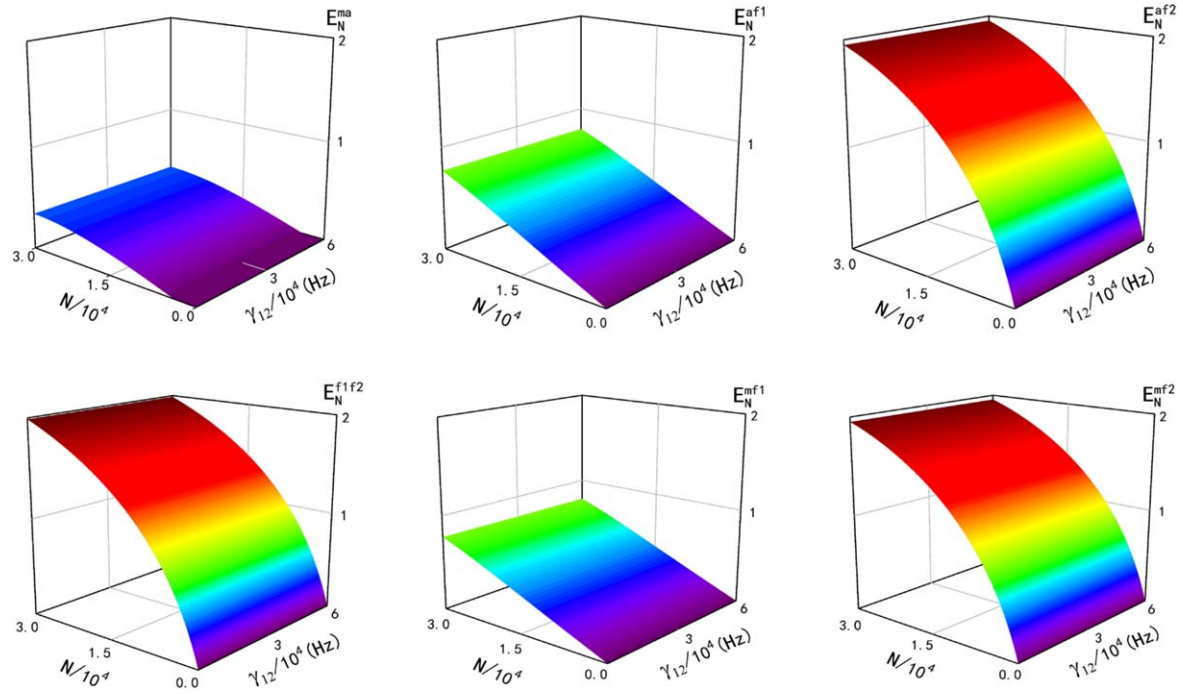

Figure 4. The 3D plots of the behavior of logarithmic negativity E_N^{ma}, $E_N^{af1(2)}$, $E_N^{mf1(2)}$, and E_N^{f1f2} with respect to the atomic ensemble number N and the coherence decay rate γ_{12} of the atomic lower doublet, where we set $\Delta_{c1} = -\Delta_{c2} = \omega_m$, and the other parameters are the same as those in figure 2(a).

modes 1 and 2, corresponding to the anti-Stokes and Stokes modes of the input fields 1 and 2, respectively, can be equivalently regarded as the result of frequency up-(or down-) conversion process through scattering the input laser fields 1 and 2 off the mechanical oscillator [24], which acts as a frequency converter with frequency equal to its oscillation frequency; since every Stokes (anti-Stokes) photon generation is always accompanied by emitting (absorbing) one mirror oscillation phonon, the cavity field 1 is quantum anti-correlated with the cavity field 2 as well as the mechanical oscillator. Note that the similar tripartite entanglement has been observed with a mechanical resonator interacting simultaneously with two cavity fields in [19, 25]. In the case that the atoms are added into the cavity, if the atoms are prepared in the coherent superposition of the lower doublet and the two-photon resonance condition is satisfied, since every photon generation of the cavity field 1 is always accompanied by annihilation of a photon of the cavity field 2 and an atomic coherence excitation, strong tripartite entanglement among the two cavity fields and the atoms can be achieved (see figure 2), where the cavity field 1 is quantum anti-correlated with the cavity field 2 as well as the atoms, which has the similar feature as the pump-signal-idler three-color entanglement produced by using an optical parametric oscillator [36, 37]. Similar strong tripartite entanglement among two laser fields and atoms has been studied in free space [8, 10]. Therefore, when the atoms prepared in the coherent superposition of the lower doublet are added into the cavity, stronger bipartite entanglement between the two cavity fields can be established as compared to that without atoms, which would result in the enhancement of the bipartite entanglement between the two cavity fields and mechanical oscillator due to the common optomechanical coupling of the two cavity fields to the mirror, and subsequent strong light–light–atom–mirror quadripartite entanglement, as shown in figure 2.

The enhancement of the tripartite entanglement among the mechanical oscillator and the two cavity fields can also be seen clearly from equations (2*a*)–(2*g*). When the atoms are added into the cavity, as seen from equations (2*c*)–(2*d*) and equations (2*f*)–(2*g*), if there is no quantum coherence between the atomic lower doublet, the existence of the atoms only has influence on the effective detunings and the decay rates of the two cavity fields; however, if the atoms are prepared in the coherent superposition of the lower doublet, except the common optomechanical coupling to the mirror oscillation mode due to radiation pressure, the two cavity field modes are further coupled with each other due to quantum coherence between the atomic lower doublet, that is, the quantum coherence between the atomic lower doublet can effectively enhance the coupling between the two cavity fields, which results in dramatic enhancement of the bipartite entanglement between the two cavity fields as compared to the case without atoms (note that the enhancement of entanglement with increasing coupling strength in a moderate range under the stability conditions in an optomechanical or atom-assisted optomechanical system has also been extensively studied [15, 25–27]). Subsequently, the enhancement of the bipartite entanglement between the two cavity fields would lead to the enhancement of the bipartite entanglement between the mechanical oscillator and cavity field 1 as well as cavity field 2 due to the common optomechanical interaction of the two cavity fields with the mirror. Also, as seen from equation (2*e*), the atomic operator σ_{21} is a linear combination of the two cavity

operators a_1 and a_2, which implies that the atoms get entangled with two cavity fields as well, thereby leading to the strong light–light–atom–mirror quadripartite entanglement. Moreover, as displayed in figure 4, dramatic enhancement of the multipartite entanglement can be achieved with increasing the atomic number N in a moderate range. Since the coupling strength between the atoms and the two cavity fields is proportional to the square root of atomic number, it clearly indicates that enhancing the coupling strength between the atoms and the two cavity fields can result in enhancing the bipartite entanglement between the two cavity fields, and subsequent multipartite entanglement.

4. Conclusion

In conclusion, we have presented a proposal to greatly enhance the tripartite entanglement among two-photon modes and the macroscopic oscillator via quantum coherence with an atom-assisted single-cavity optomechanical system. Moreover, strong quadripartite entanglement among the two cavity modes and the mirror oscillation mode as well as the atoms can be obtained due to the common coupling of the two cavity fields to both the mirror and atoms. The present atom-assisted optomechanical system represents an alternative useful tool for the realization of quantum interface, able to perform quantum state exchange between light and light, light and matter, as well as one matter and another matter, which may find potential applications in realistic quantum information processing and quantum networks.

Acknowledgments

This work is supported by National Science Foundation of China (Nos. 11574195, and 61435007), Innovation Action Plan of International Academic Cooperation and Exchange Program of Shanghai Municipal Science and Technology Commission (No. 16520720800), Shanghai Natural Science Foundation (14ZR1415400). Yang's e-mail is yangxh@shu.edu.cn or yangxih1@yahoo.com.

ORCID iDs

Xihua Yang https://orcid.org/0000-0003-3430-3061
Min Xiao https://orcid.org/0000-0001-9207-0927

References

[1] Bouweester D, Ekert A and Zeilinger A 2000 *The Physics of Quantum Information* (Berlin: Springer)
[2] Nielsen M A and Chuang I L 2000 *Quantum Computation and Quantum Information* (Cambridge: Cambridge University Press)
[3] Kimble H J 2008 The quantum internet *Nature* **453** 1023–30
[4] Pan J W, Chen Z B, Lu C Y, Weinfurter H, Zeilinger A and Żukowsk M 2012 Multiphoton entanglement and interferometry *Rev. Mod. Phys.* **84** 777–838
[5] Kuzmich A, Bowen W P, Boozer A D, Boca A, Chou C W, Duan L M and Kimble H J 2003 Generation of nonclassical photon pairs for scalable quantum communication with atomic ensembles *Nature* **423** 731–4
[6] Boyer V, Marino A M, Pooser R C and Lett P D 2008 Entangled images from four-wave mixing *Science* **321** 544–7
[7] Sangouard N, Simon C, de Riedmatten H and Gisin N 2011 Quantum repeaters based on atomic ensembles and linear optics *Rev. Mod. Phys.* **83** 33–80
[8] Yang X H, Xue B L, Zhang J X and Zhu S Y 2014 A universal quantum information processor for scalable quantum communication and networks *Sci. Rep.* **4** 6629
[9] Yang X H, Zhou Y Y and Xiao M 2012 Generation of multipartite continuous-variable entanglement via atomic spin wave *Phys. Rev.* A **85** 052307
[10] Yang X H and Xiao M 2015 Electromagnetically induced entanglement *Sci. Rep.* **5** 13609
[11] Genes C, Mari A, Vitali D and Tombesi P 2009 Quantum effects in optomechanical systems *Adv. At., Mol., Opt. Phys.* **57** 33–86
[12] Aspelmeyer M, Kippenberg T J and Marquardt F 2014 Cavity optomechanics *Rev. Mod. Phys.* **86** 1391–452
[13] Meystre P 2013 A short walk through quantum optomechanics *Ann. Phys.* **525** 215–33
[14] Genes C, Vitali D and Tombesi P 2008 Emergence of atom–light–mirror entanglement inside an optical cavity *Phys. Rev.* A **77** 050307
[15] Ian H, Gong Z R, Liu Y X, Sun C P and Nori F 2008 Cavity optomechanical coupling assisted by an atomic gas *Phys. Rev.* A **78** 013824
[16] Hammerer K, Aspelmeyer M, Polzik E S and Zoller P 2009 Establishing Einstein–Poldosky–Rosen channels between nanomechanics and atomic ensembles *Phys. Rev. Lett.* **102** 020501
[17] Zhou L, Han Y, Jing J T and Zhang W P 2011 Entanglement of nanomechanical oscillators and two-mode fields induced by atomic coherence *Phys. Rev.* A **83** 052117
[18] Benguria R and Kac M 1981 Quantum Langevin equation *Phys. Rev. Lett.* **46** 1–4
[19] Paternostro M, Vitali D, Gigan S, Kim M S, Brukner C, Eisert J and Aspelmeyer M 2007 Creating and probing multipartite macroscopic entanglement with light *Phys. Rev. Lett.* **99** 250401
[20] Vitali D, Gigan S, Ferreira A, Böhm H R, Tombesi P, Guerreiro A, Vedral V, Zeilinger A and Aspelmeyer M 2007 Optomechanical entanglement between a movable mirror and a cavity field *Phys. Rev. Lett.* **98** 030405
[21] Adesso G, Serafini A and Illuminati F 2004 Extremal entanglement and mixedness in continuous variable systems *Phys. Rev.* A **70** 022318
[22] Wang Y D and Clerk A 2013 Reservoir-engineered entanglement in optomechanical systems *Phys. Rev. Lett.* **110** 253601
[23] Kuzyk M C, van Enk S J and Wang H 2013 Generating robust optical entanglement in weak-coupling optomechanical systems *Phys. Rev.* A **88** 062341
[24] Yang X H, Ling Y, Shao X P and Xiao M 2017 Generation of robust tripartite entanglement with a single-cavity optomechanical system *Phys. Rev.* A **95** 052303
[25] Barzanjeh S, Vitali D, Tombesi P and Milburn G J 2011 Entangling optical and microwave cavity modes by means of a nanomechanical resonator *Phys. Rev.* A **84** 042342
[26] Genes C, Mari A, Tombesi P and Vitali D 2008 Robust entanglement of a micromechanical resonator with output optical fields *Phys. Rev.* A **78** 032316
[27] Genes C, Ritsch H, Drewsen M and Dantan A 2011 Atom-membrane cooling and entanglement using cavity electromagnetically induced transparency *Phys. Rev.* A **84** 051801

[28] Tian L 2013 Robust photon entanglement via quantum interference in optomechanical interfaces *Phys. Rev. Lett.* **110** 233602
[29] Mancini S, Giovannetti V, Vitali D and Tombesi P 2002 Entangling macroscopic oscillators exploiting radiation pressure *Phys. Rev. Lett.* **88** 120401
[30] Pirandola S, Mancini S, Vitali D and Tombesi P 2003 Continuous-variable entanglement and quantum-state teleportation between optical and macroscopic vibrational modes through radiation pressure *Phys. Rev.* A **68** 062317
[31] Wu H B and Xiao M 2014 Strong coupling of an optomechanical system to an anomalously dispersive atomic medium *Laser Phys. Lett.* **11** 126003
[32] Chen Y B 2013 Macroscopic quantum mechanics: theory and experimental concepts of optomechanics *J. Phys. B: At. Mol. Opt. Phys.* **46** 104001
[33] Parks P C and Hahn V 1993 *Stability Theory* (New York: Prentice-Hall)
[34] Vidal G and Werner R F 2002 Computable measure of entanglement *Phys. Rev.* A **65** 032314
[35] Gröblacher S, Hammerer K, Vanner M R and Aspelmeyer M 2009 Observation of strong coupling between a micromechanical resonator and an optical cavity field *Nature* **460** 724–7
[36] Villar A S, Martinelli M, Fabre C and Nussenzveig P 2006 Direct production of tripartite pump-signal-idler entanglement in the above-threshold optical parametric oscillator *Phys. Rev. Lett.* **97** 140504
[37] Coelho A S, Barbosa F A S, Cassemiro K N, Villar A S, Martinelli M and Nussenzveig P 2009 Three-color entanglement *Science* **326** 823–6